CHANGES IN THE CRITICAL FREQUENCY *foF*2 AND THEIR INTERPRETATION

© 2025 A. D. Danilov[a, *], N. A. Berbeneva[b]

[a]*Fedorov Institute of Applied Geophysics, Moscow, Russia*

[b]*Physics Faculty of M.V. Lomonosov Moscow State University, Moscow, Russia*

**e-mail: adanilov99@mail.ru*

Received January 10, 2025

Revised February 09, 2025

Accepted April 14, 2025

Abstract. The results of the recent publication by Qiann and Mursula who have found an increase with time in the ratio of the modelled and observed values of the thermospheric density at satellite heights are considered. It is assumed that that increase is related to the existence of the negative trend in the density that is not described by the model properly. To confirm this concept, the change with time in the modelled and observed values of the *F*2-layer critical frequency *foF*2, *foF*2(mod)/*foF*2(obs) based on the observations at the Northern and Southern hemisphere stations is considered. It is shown that the same increase is observed for this ratio as for the ratio of densities. It is found that the rate of this increase in *foF*2 correlate well with the *foF*2 trends (in MHz/year) in winter months when the negative trends are small. In the winter months when the *foF*2 trends are small, there is almost no *foF*2(mod)/*foF*2(obs) increase. All that allows us to assume that the results of Qiann and Mursula show that the model incompletely describes the negative trends in the density.

Keywords: *trends in thermospheric density, ratio of observed and modelled values of foF2, seasonal variations*

DOI: 10.31857/S00167940250408e4

1. INTRODUCTION

The problem of choosing the best solar activity index (SA) for describing the behavior with time of ionospheric parameters is well known. It is very important, including for the problem of analyzing the changes of the thermosphere and ionosphere parameters during the last decades. First of all, it concerns finding the long-term trends of the thermospheric gas density, as well as the critical frequency foF2 and the height hmF2 of *the* F2 layer. More details can be found in the reviews by Laštovička [2023] and Cnossen et al. [2024].

A recent paper by Qiann and Mursula [2024] discusses in detail how the known CA indices *F10*.7 and F30 describe the change with time of the thermospheric density at an altitude of 400 km. The authors compare the observed change in densityρ with calculations of this change using the TIME-GCM model developed and modernized at NCAR (Boulder, USA). The observed change ofρ with time at the indicated altitude is taken from the analysis of more than 7700 satellite orbits from [Emmert et al., 2021].

The main emphasis in Qiann and Mursula [2024] is on comparing the description of changesρ using the *F10*.7 and F30 indices. The main conclusion of this part of the paper is that the *F30* index better describes the change in the amount of energy contributed by solar radiation to the thermosphere than the *F10*.7 index. However, the authors also make some conclusions about the long-term trendsρ , which are of interest for this paper.

Figure 1.

Adapted Figure 1, taken from the above paper, shows the change in the ratio of modeled (using the *F30* index) to observed density values (labeled asρ_{model}/ρ_{data}) for the two periods. Several details of this figure are of interest. First, it can be seen that the ratioρ_{model}/ρ_{data} increases with time. This, in our view, indicates that there is a well-defined trendρ . Second, we can see that this change in the observed values relative to the linear approximation has a wavy character and correlates well with the change in the CA index *F10*.7. We will discuss these features in detail below.

It seems to us that the well-defined and statistically significant increase in the ratioρ_{model}/ρ_{data} is direct evidence of a negative density trendρ . Indeed, if the model gives a correct description of what should be (which is apparently the best model to date), then an increase inρ_{model}/ρ_{data} can only mean a decrease in the real (observed) density with time, in other words, a negative density trendρ

However, Qiann and Mursula [2024] point out that the model includes an increase in CO_2 due to anthropogenic effects according to measurements at Obs. Mauna Loa (USA). But Fig. 1 shows that the difference between model values and observed values increases with time, which, in our opinion, means that the model predicts smaller trendsρ , than those that exist in reality. According to Qiann and

Mursula [2024] the model is not perfect enough because it uses the *F10*.7 index to describe CA effects. They believe that a model using the F30 index would give better agreement with observations, since their main result is precisely that the F30 index better describes CA effects than the *F10*.7 index.

The wavy change ofρ_{model}/ρ_{data} with time in Fig. 1 with excellent correlation with the SA index indicates, in our opinion, only that the trends ofρ depend on solar activity. But this is exactly what is actually observed from satellite orbit data - the negative trends ofρ are maximal at minimum SA (~7%) and minimal at high SA (~2%) [Solomon et al., 2018].

In this paper, a study similar to the study of Qiann and Mursula [2024], but for long-term changes in the critical frequency of the F2 layer, *foF2*, is carried out. Trends of foF2, *k*(*foF2*), from vertical sounding data at several ionospheric stations were considered in a number of papers of our group [Danilov et al., 2024; 2025; Danilov and Ryabukhin, 2025]. We use the calculations performed there for trend calculation to construct figures similar to Fig. 1.

Since Qiann and Mursula [2024] compare model and observed values, we analyze a similar relation for *foF2*. As a model, we use the dependence of *foF2* on solar activity for the period we call "reference", assuming that in this period there were no trends of ionospheric parameters of anthropogenic nature yet. To make the analysis more complete, we do it for three SA indices (*F30*, Ly-α and *MgII*), which, according to many researchers, are the best for describing the dependence of ionospheric parameters on SA.

2. DATA ANALYSIS FOR ST. JULIUSRUH

For this station, we performed the calculations in a way that is closest to the calculations of Qiann and Mursula [2024]. We used the values of foF2(mod) and foF2(nab) from our previous publications on *foF2* trends [Danilov et al., 2024; 2025; Danilov and Ryabukhin, 2025]. The first analyzed interval was the period from 1967 (exactly as in Qiann and Mursula [2024]) to the present (2016 for them and 2022/2024 for us). For this period, we plotted the *foF2*(mod)/*foF2*(nab) dependence on time, similar to theρ_{model}/ρ_{data} dependence in Qiann and Mursula [2024]. Similar to that work, we obtained the slope of the approximating line, which we denoted as *L*. We analyzed two winter months and five near-midday LT moments (when we assume foF2 trends are maximal). Examples of *foF2*(mod)/*foF2*(nab) changes for the period 1967-2023 for January and February are shown in Fig. 2 and Fig. 3, respectively.

Figure 2.

Figure 3.

As it follows from these figures, for all considered situations (LT moment, CA index) there is an increase in the value of *foF2*(mod)/*foF2*(nab) with time. Although the spread of points is quite large, the R^2 values (certainty coefficient by Fisher's F-test) given in the figures show that all dependencies

are statistically significant. For a given number of points (49), the statistical significance *S of* the resulting dependencies is 99 and 98% with R^2= 0.5 and 0.3, respectively.

We believe that the significant scatter of points in Fig. 2 and Fig. 3 is due (apart from the inevitable variation in the values of the monthly medians foF2(nab) used for the analysis) mainly to the fact that the points for the reference period, when there were no trends, and for later years, when trends should change the observed values of *foF2*, are analyzed together. To test this assertion, we plotted the same plots for the later period 2001-2023, when it is our firm belief that negative trends in the daytime hours of the winter months exist. Examples are shown in Fig. 4 and Fig. 5.

Figure 4.

Figure 5.

A summary of the results of determining the *L* values from data of station Juliusruh for January and February is presented in Table 1 and Table 2, respectively. The *L* values for each of the five LT midday hours at each of the three SA indices are presented there. The penultimate column gives the *L* value for the relationship of *foF2*(mod)/*foF2*(nab) values averaged over all five LTs. The last column gives the result of averaging these values over all three CA indices.

Table 1.

Table 2.

Figures 2-5 and Tables 1 and 2 show that in all cases there is a better or worse pronounced increase of *foF2*(mod)/*foF2*(nab) with time, and the value of *L* is positive. One can see a large difference in the dependence of the *foF2*(mod)/*foF2*(nab) value on time for the two intervals considered. First of all, the scatter of points relative to the approximating lines is much stronger for 1967-2023 than for 2001-2023. This is also reflected in the R^2 values shown in the figures and tables. As noted above, we believe that this difference is due to the fact that in the case of the first interval, points for years that have not yet had *foF2* trends are included in the analysis. And in the case of the second interval, we analyze points for years in which we believe negative *foF2* trends were present. As in the case ofρ_{model}/ρ_{data} values discussed above, we believe that the increase over time of the *foF2*(mod)/*foF2*(nab) ratio (positive *L* values) demonstrates the presence of a negative foF2 trend: for each fixed CA index value, the foF2(mod) value remains constant, while the *foF2*(nab) value decreases over the years due to the presence of a negative *foF2* trend

An important factor is the difference in the *L* values obtained for the two periods - these values are significantly larger for 2001-2023 than for 1967-2023. The reason, in our opinion, is the same**:** first period includes years when there were no trends yet, while the second covers years when there were trends. We will return to this issue below. Tables 1 and 2 show that the resulting LT-averaged *L* values for a given month but different CA indices are close to each other for the earlier period. In January,

these are 0.00253, 0.00310 and 0.00199 for F30, Ly-α and *MgII*, respectively. The same values in February are 0.00137, 0.00106 and 0.00117.

Table 3.

As noted above, Fig. 1 draws attention to the fact that deviations ofρ_{model}/ρ_{data} from the approximating line have a wavy character and show a clear dependence on SA. This reflects the dependence of the thermospheric density trends on solar activity. We checked to what extent the *foF2*(mod)*/foF2*(nab) values we obtain correlate with the CA indices. Table 3 shows as an example the R^2 values for the dependences of the calculated *foF2*(mod)*/foF2*(nab) values on the CA indices for several situations. It can be seen that the R^2 values in Table 3 are very small, indicating that there is no significant relationship between *foF2*(mod)*/foF2*(nab) and CA indices. Exactly the same pattern is observed for all the situations considered in this paper. This is consistent with our previous results that *foF2* trends (unlikeρ) do not show a significant dependence on CA.

3. RESULTS FOR OTHER STATIONS

In order not to overload the article with tables and graphs, we present the results of determining the *L* values for the stations for which we published the results of foF2 trends determination only for the later period 2001-2023/2024, when these trends were known to exist. Examples of changes with time of *foF2*(mod)*/foF2*(nab) values for Moscow and Sverdlovsk stations are given in Fig. 6. 6.

Figure 6.

Table 4.

Table 5.

Tables 4 and 5 present as an example the results of *L* determination for all five near-midday LT moments for January at Sverdlovsk station and for February at Moscow station, respectively. Tables 4 and 5 show that in both considered examples, for all LT, the values of *L* are observed for all LT, which within each specific situation (station, CA index, month) are quite close. The LT average *L* values for specific stations and month are also quite close in order of magnitude. Finally, the average *L* values for all LT and all CA indices in the two examples considered differ by a factor of less than 1.5.

For Boulder station and three stations of the Southern Hemisphere, which were considered in our previous studies, we present a comparison of the *L* values obtained for each SA index and month by averaging the *foF2*(mod)*/foF2*(nab) values for all five LT moments. For Boulder station, the same two winter months of January and February were considered, while the winter month of June was considered for Townsville, Hobart, and Canberra stations. The results are summarized in Table 6. Figure 6 and Tables 4-6 show that the same pattern is observed for all stations considered as for the Juliusruh station data analyzed in detail in the previous paragraph. The values of *L*, although differing for different situations, mainly lie in the interval 0.00400-0.00700. The vast majority of the obtained

values of L have rather high statistical significance, since the corresponding values of R^2 are rather high

Figure 6.

4. DISCUSSION

The purpose of this paper is to analyze the change in the ratio of model and observed foF2 values with time, similar to the analysis of changes inρ_{model}/ρ_{data} in Qian and Ursula [2024]. Our main postulate is that the growth of theρ_{model}/ρ_{data} ratio in Fig. 1, taken from Qian and Ursula [2024], is a reflection of the existence of long-term trendsρ, that are well known from observations of satellite orbital evolution. The fact that the deviations ofρ_{model}/ρ_{data} in Fig. 1 from the approximating line have a wave-like character and correlate well with the CA index, F10.7, in our opinion, confirm this postulate, since the dependence ofρ trends on CA is well known. In our analysis we obtained approximately the same picture for the change with time of *foF2*(mod)*/foF2*(nab)

The most detailed analysis performed for Juliusruh station (paragraph 2) showed that when considering the same time interval (from 1967 to the present) as in Qian and Ursula [2024], we observe an increase in the value of *foF2*(mod)*/foF2*(nab) with time, but the values of the slope of the approximating line L and the certainty coefficient R^2, showing the statistical significance of the obtained dependences, are relatively small. We attribute this to the fact that the specified time interval includes years when foF2 trends were not yet present, or they were very small.

For the later time interval 2001-2023/2024, when, according to our ideas, *foF2* trends were known to exist, the pattern of *foF2*(mod)*/foF2*(nab) changes becomes much more pronounced - both L and R^2 values increase significantly.

As shown in paragraph 3, the same pattern of *foF2*(mod)*/foF2*(nab) variation with time during the 2001-2023/24 interval is observed for the other five analyzed stations in the Northern and Southern Hemispheres

To illustrate our claim that the values of the slope L (the ratio$\rho_{(model)}/\rho_{data}$ in the case of the work of Qian and Ursula [2024] and the ratio *foF2*(mod)*/foF2*(nab) in our case) are a reflection of the existence of trends, we compared the values of the trends foF2, k(*foF2*) obtained in the works of Danilov et al. [2024; 2025] with the L values obtained in this work for the same stations and the same months. Although one cannot expect a 100% correlation, since the procedures for analyzing the dependences ofΔ *foF2* (in determining trends) and *foF2*(mode)*/foF2*(nab) on time are somewhat different, it turned out that in all cases there is a positive correlation between the trend amplitude and the L value. In other words, the stronger the negative trend of foF2, the larger the value of L

Figure 7.

As an example, we present in Fig. 7 the relationship between L and $k(foF2)$ for winter months for Boulder (Northern Hemisphere) and Townsville (Southern Hemisphere) stations. Each point corresponds to the values of $k(foF2)$ and L for the same LT moment and CA index. It can be seen that the positive relationship between these parameters is well pronounced and statistically significant. We believe that this is a confirmation of our main postulate that the value of L in both the case ofρ_{model}/ρ_{data}, and in the case of $foF2$(mod)/$foF2$(nab) indicates the presence ofρ and foF2 trends, respectively

To further confirm this postulate, we analyzed the L values for the summer months, when, according to our data (see Danilov et al. [2024; 2025]), $foF2$ trends are practically absent. As we expected, the L values turned out to be very small. As an example, we present in Table 7 the values of L and R^2 for winter months for two stations (one from the Northern and one from the Southern Hemispheres). As can be seen from this table, the values of L are very small in the summer months compared to the corresponding values in the winter months. This is fully consistent with our ideas that foF2 trends are practically absent in summer. The very small values of R^2 show that the resulting L values are not really significant. The presence of both negative and positive values of L in summer months (and in winter months only positive L values are obtained) is in perfect agreement with the fact that in summer months the $foF2$ trends are not only small in amplitude, but also change sign.

4. CONCLUSION

Qiann and Mursula [2024] analyzed the time dependence of the ratio$\rho_{model}/\rho_{(data)\ of}$ the thermospheric densitiesρ, calculated by the TIME-GCM model and obtained from satellite orbit evolution observations. The results of this analysis, shown in Fig. 1, borrowed from this paper, show, our opinion, that there is a density trend that is not fully described by the model

We performed a similar analysis for the ratio of model and observed values of the critical frequency $foF2$, $foF2$(mode)/$foF2$(nab) for a number of VZ stations for two periods. For the same period analyzed by Qiann and Mursula [2024] (from 1967 to the present) we obtained a trend of increasing $foF2$(mod)/$foF2$(nab) with time, similar to the increase ofρ_{model}/ρ_{data} in Fig. 1, but with a larger scatter of points relative to the approximating line. We believe that this is due to the fact that the analyzed period includes also earlier years when there were no $foF2$ trends yet.

For the later period 2001-2022/2024, we obtained a much better pronounced growth of $foF2$(mod)/$foF2$(nab) with time. The slope L *of* the line approximating the indicated growth increased sharply. This was the first confirmation of our concept that the slope of L *is* related to foF2 trends, since we believed that $foF2$ trends already existed during this period. At the same time, we indirectly confirmed the existence of negative foF2 trends in recent decades.

To further confirm this concept, we compared the L values obtained in this work with the trends of foF2, $k(foF2)$ obtained in our previous publications [Danilov et al., 2024; 2025; Danilov and

Ryabukhin, 2025] for the same conditions (stations, CA indices, LT moments). It turned out that there is a well-defined and statistically significant correlation between the values of L and k(*foF2*).

Finally, we analyzed a similar time dependence of *foF2*(mod)/*foF2*(nab) values for the summer months, when, according to our data, *foF2* trends are very small. As we expected, we obtained very small and statistically insignificant values of L for summer.

All this allows us to consider that the values ρ_{model}/ρ_{data} in Qiann and Mursula [2024] and the values *foF2*(mod)/*foF2*(nab) in this paper reflect the presence of negative trends in the thermospheric density and critical frequency of the *F2* layer, respectively.

ACKNOWLEDGEMENTS

The values of *foF2*(mod)/*foF2*(nab) analyzed in this paper were taken from our previous publications [Danilov et al., 2024; 2025; Danilov and Ryabukhin, 2025], which provide references to sites where the corresponding values of foF2 critical frequencies are given.

REFERENCES

1. *Danilov A.D., Konstantinova A.V., Berbeneva N.A.* Trends of the critical frequency *foF2* from data of the stations of the Northern and Southern Hemispheres // Geomagnetism and Aeronomy. T. 64. № 3. C. 387-400. 2024. https://doi.org/10.31857/S0016794024030059

2. *Danilov A.D., Konstantinova A. V., Ryabukhin I.A. V., Ryabukhin I. A.* Trends of the *F2* layer parameters from data of Sverdlovsk station (Arti) // Geomagnetism and Aeronomy T. 65. № 4. P. . 2025.

3. *Cnossen I., Emmert J.T. Garcia R.R., Elias A.G., Mlynczak M.G., Zhang Sh.R.*. A review of global long-term changes in the mesosphere, thermosphere and ionosphere: a starting point for inclusion in (semi-)empirical models // Adv. Space Res. V. 74. N 11. P. 5991-6011. 2024. https://doi.org/10.1016/j.asr.2024.10.005

4. *Danilov A.D., Ryabukhin I.A.* Trends of the *F2-layer* parameters based on Sverdlovsk (Arti) station data // Adv. Space Res. 2025. https://doi.org/10.1016/j.asr.2024.12.078

5. *Emmert J.T., Dhadly M.S., Segerman* A.*M.* A globally averaged thermospheric density data set derived from two-line orbital element sets and special perturbations state vectors // J. Geophys. Geophys. Res. - Space. V. 126. N 8. ID e2021JA029455. 2021. https://doi.org/10.1029/2021JA029455

6. *Laštovička J.* Progress in investigating long-term trends in the mesosphere, thermosphere, and ionosphere // Atmos. Chem. Phys. V. 23. N 10. P. 5783-5800. 2023. https://doi.org/10.5194/acp-23-5783-2023

7. *Qian L., Mursula K.* Evaluating *F10*.7 and F30 radio fluxes as long-term solar proxies of energy deposition in the thermosphere // Ann. Gophys. Discuss. 2024. https://doi.org/10.5194/angeo-2024-23

8. Solomon S., Liu H., Marsh D., McInerney J., Qian L., Vitt F. Whole atmosphere simulation of anthropogenic climate change // Paper presented at the 10th Workshop on Long-Term Changes and Trends in the Atmosphere. May 14-18, 2018. Hefei, China. 2018.

Table 1. Values of the slope of the approximating line *L* for January (Juliusruh station)

Parameter	Measurement interval	10 LT	11 LT.	12 LT.	13 LT.	14 LT	LT average	Average by indices
F30								
L	1967-2023	0.00221	0.00257	0.00260	0.00292	0.00276	0.00253	–
R^2	1967-2023	0.38	0.45	0.54	0.54	0.50	0.56	–
L	2001-2023	0.00148	0.00367	0.00407	0.00404	0.00791	0.0375	–
R^2	2001-2023	0.03	0.18	0.27	0.24	0.65	0.25	–
Ly-α								
L	1967-2023	0.00244	0.00307	0.00283	0.00319	0.00308	0.00310	0.00304
R^2	1967-2023	0.43	0.46	0.48	0.44	0.50	0.54	–
L	2001-2023	0.00248	0.00565	0.00526	0.00528	0.00673	0.00491	0.00551
R^2	2001-2023	0.07	0.29	0.23	0.32	0.42	0.32	–
MgII								
L	1967-2023	0.00156	0.00216	0.00192	0.00221	0.00196	0.00199	–
R^2	1967-2023	0.24	0.41	0.36	0.39	0.32	0.49	–
L	2001-2023	0.00325	0.00620	0.00581	0.00585	0.00636	0.00603	–
R^2	2001-2023	0.17	0.53	0.52	0.46	0.56	0.62	–

Table 2. Values of the slope of the approximating line L for February (Juliusruh station)

L, R^2	Measurement interval	10 LT	11 LT.	12 LT.	13 LT.	14 LT	LT average	Average by indices
F30								
L	1967-2023	0.00102	0.00110	0.00121	0.00170	0.00190	0.00137	–
R^2	1967-2023	0.04	0.05	0.09	0.17	0.32	0.12	–
L	2001-2023	0.00598	0.00799	0.00619	0.00585	0.00711	0.0654	–
R^2	2001-2023	0.41	0.	0.57	0.40	0.56	0.59	–
Ly-α								
L	1967-2023	0.00175	0.00185	0.00201	0.00244	0.00259	0.00106	0.00129
R^2	1967-2023	0.11	0.12	0.15	0.22	0.36	0.19	–
L	2001-2023	0.00558	0.00961	0.00638	0.00641	0.00789	0.00683	0.00551
R^2	2001-2023	0.23	0.60	0.30	0.26	0.49	0.37	–
MgII								
L	1967-2023	0.00080	0.00084	0.00132	0.00136	0.00170	0.00117	–
R^2	1967-2023	0.03	0.04	0.10	0.11	0.29	0.09	–
L	2001-2023	0.00627	0.00796	0.00711	0.00636	0.00757	0.00705	–
R^2	2001-2023	0.53	0.75	0.66	0.46	0.71	0.73	–

Table 3: Values of R^2 (Juliusruh st.)

LT	Parameter			
	Ly-α February	Ly-α Jan.	F30 February	F30 January
10:00	0.09	0.03	0.10	0.04
11:00	0.06	0.02	0.05	0.00
12:00	0.05	0.02	0.03	0.04
13:00	0.07	0.02	0.05	0.04
14:00	0.08	0.02	0.07	0.04
all LT	0.08	0.03	0.09	0.03

Table 4. Parameter *L* values for January (Svedlovsk station)

Parameter	10 LT	11 LT.	12 LT	13 LT.	14 LT	Average on LT	by indices
F30							
L	0.00282	0.00416	0.00372	0.00331	0.00369	0.00354	–
R^2	0.07	0.19	0.16	0.17	0.18	0.20	–
Ly-α							
L	0.00394	0.00551	0.00513	0.00470	0.00483	0.00483	0.00449
R^2	0.10	0.24	0.23	0.21	0.24	0.27	–
MgII							
L	0.00445	0.00580	0.00525	0.00490	0.00509	0.00510	–
R^2	0.26	0.36	0.38	0.58	0.40	0.53	–

Table 5. Values of parameter *L* for February (st. Moscow)

Parameter	10 LT	11 LT.	12 LT.	13 LT.	14 LT	Average on LT	Average by indices
F30							
L	0.00627	0.00570	0.00594	0.00563	0.	0.00591	–
R^2	0.42	0.42	0.54	0.39	0.36	0.49	–
Ly-α							
L	0.00551	0.00553	0.00563	0.00554	0.00598	0.00564	0.00672
R^2	0.30	0.37	0.37	0.26	0.32	0.37	–
MgII							
L	0.00973	0.00935	0.00856	0.00589	0.00586	0.00861	–
R^2	0.36	0.28	0.25	0.11	0.13	0.25	–

Table 6: *L* values averaged over LT for winter

Parameter	Boulder		Townsville	Hobart	Canberra
	January	February	June	June	June
F30					
L	0.00307	0.00622	0.00510	0.00442	0.00510
R^2	0.11	0.33	0.40	0.29	0.40
Ly-α					
L	0.00781	0.00836	0.00488	0.00509	0.00488
R^2	0.50	0.40	0.41	0.53	0.41
MgII					
L	0.00491	0.00903	0.00667	0.00713	0.00667
R^2	0.24	0.25	0.37	0.26	0.37
Average 3					
L	0.00526	0.00787	0.00555	0.00555	0.00555

Table 7. *L* values for Hobart (February) and Sverdlovsk (July) stations

Parameter	10 LT	11 LT.	12 LT.	13 LT.	14 LT	Average on LT	Average by indices
Hobart (February).							
F30							
L	0.00172	0.00312	0.00280	0.00227	0.00207	0.00267	–
R^2	0.046	0.117	0.118	0.092	0.064	0.121	–
Ly-α							
L	0.00177	0.00210	0.00159	0.00240	0.00199	0.00203	0.00209
R^2	0.031	0.050	0.032	0.072	0.049	0.053	–
MgII							
L	0.00134	0.00181	0.00108	0.00181	0.00174	0.00157	–
R^2	0.010	0.019	0.007	0.021	0.023	0.016	–
Sverdlovsk (July)							
F30							
L	0.00067	0.00031	−0.00023	−0.00027	0.00053	−0.00058	–
R^2	0.010	0.002	0.002	0.002	0.005	0.016	–
Ly-α							
L	0.00074	−0.00069	0.00023	0.00092	−0.00057	0.00027	− 0.00002
R^2	0.022	0.012	0.001	0.011	0.005	0.002	–
MgII							
L	0.00124	0.00073	0.00134	0.00155	0.00245	0.00092	–
R^2	0.063	0.019	0.046	0.034	0.128	0.038	–

FIGURE CAPTIONS

Fig. 1. Variation ofρ_{model}/ρ_{data} ratio with time according to Qiann and Mursula [2024].

Fig. 2. Examples of the variation with time of *foF2*(mod)/*foF2*(nab) for 1967-2023 (January, Juliusruh station).

Fig. 3. Examples of the variation with time of *foF2*(mod)/*foF2*(nab) for 1967-2023 (February, Juliusruh station).

Fig. 4. Examples of the variation with time of *foF2*(mod)/*foF2*(nab) for 2001-2023 (January, Juliusruh station).

Fig. 5. Examples of the variation with time of *foF2*(mod)/*foF2*(nab) for 2001-2023 (February, Juliusruh station).

Fig. 6. Examples of *foF2*(mod)/*foF2*(nab) variation with time for Moscow and Sverdlovsk stations.

Fig. 7. Examples of the relationship between the *foF2* trend, *k*(foF2), and the parameter *L* for two stations.

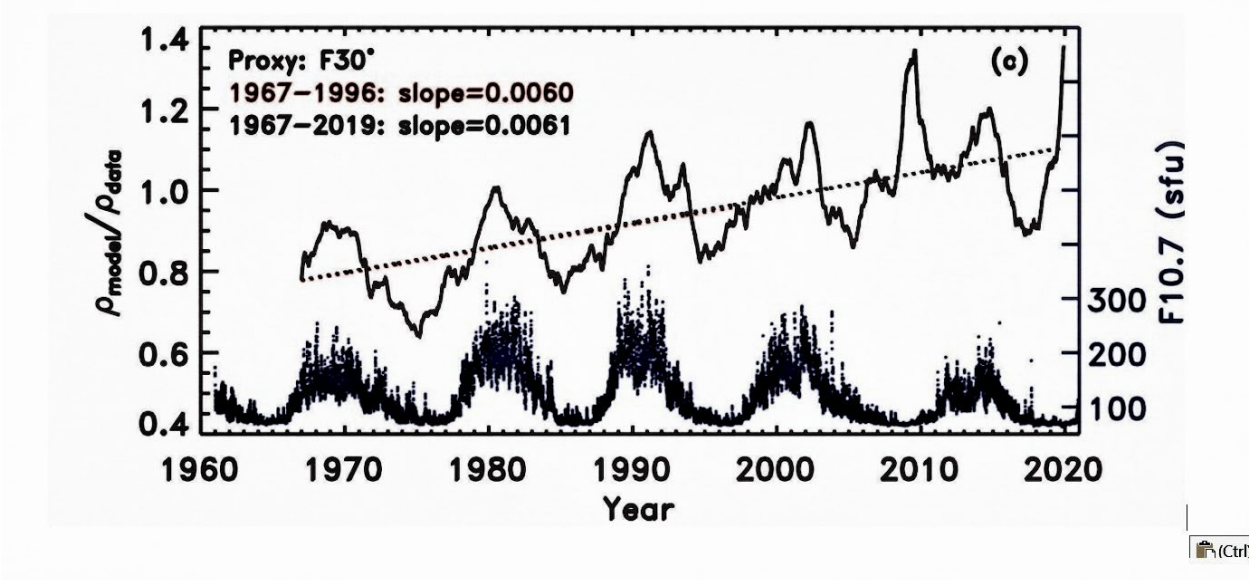

Fig. 1.

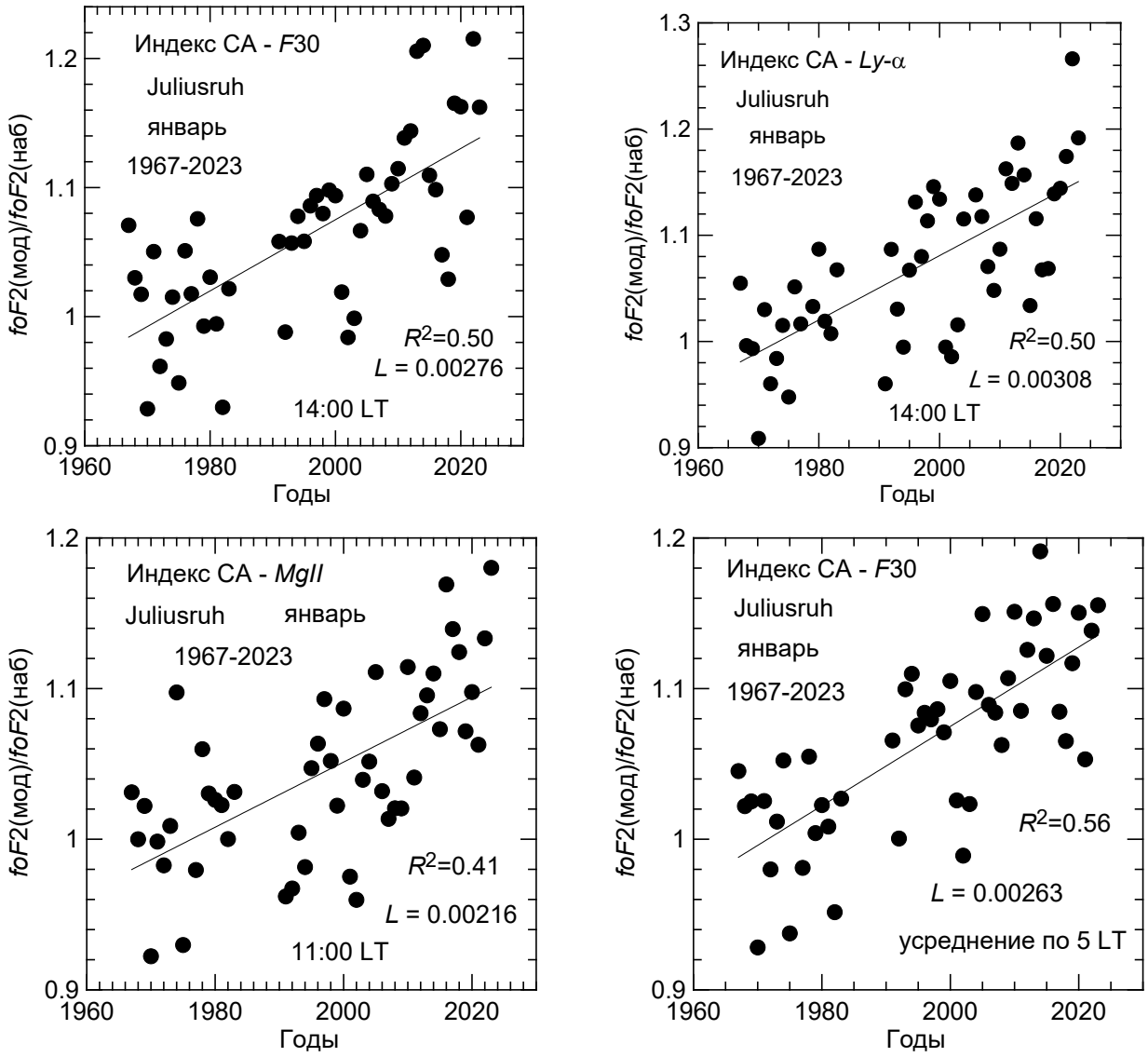
Индекс СА - F30
Juliusruh
январь
1967-2023
R2=0.50
L = 0.00276
14:00 LT
foF2(мод)/foF2(наб)
Годы
Индекс СА - Ly-α
Juliusruh
январь
1967-2023
R2=0.50
L = 0.00308
14:00 LT
foF2(мод)/foF2(наб)
Годы
Индекс СА - MgII
Juliusruh
январь
1967-2023
R2=0.41
L = 0.00216
11:00 LT
foF2(мод)/foF2(наб)
Годы
Индекс СА - F30
Juliusruh
январь
1967-2023
R2=0.56
L = 0.00263
усреднение по 5 LT
foF2(мод)/foF2(наб)
Годы

Fig. 2.

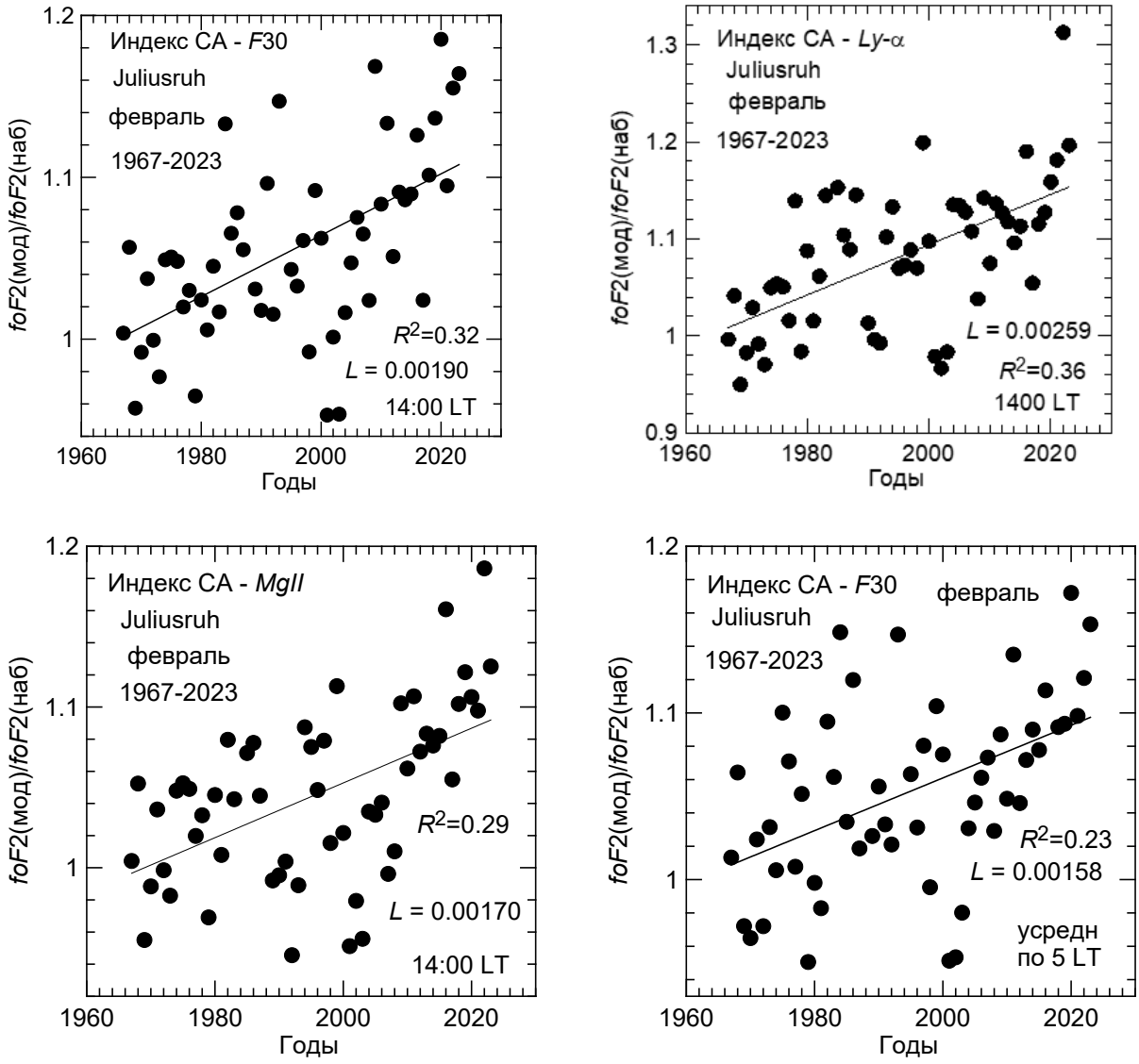
Индекс СА - F30
Juliusruh
февраль
1967-2023
R2=0.32
L = 0.00190
14:00 LT
foF2(мод)/foF2(наб)
Годы
Индекс СА - Ly-α
Juliusruh
февраль
1967-2023
L = 0.00259
R2=0.36
1400 LT
foF2(мод)/foF2(наб)
Годы
Индекс СА - MgII
Juliusruh
февраль
1967-2023
R2=0.29
L = 0.00170
14:00 LT
foF2(мод)/foF2(наб)
Годы
Индекс СА - F30
Juliusruh
февраль
1967-2023
R2=0.23
L = 0.00158
усредн
по 5 LT
foF2(мод)/foF2(наб)
Годы

Fig. 3.

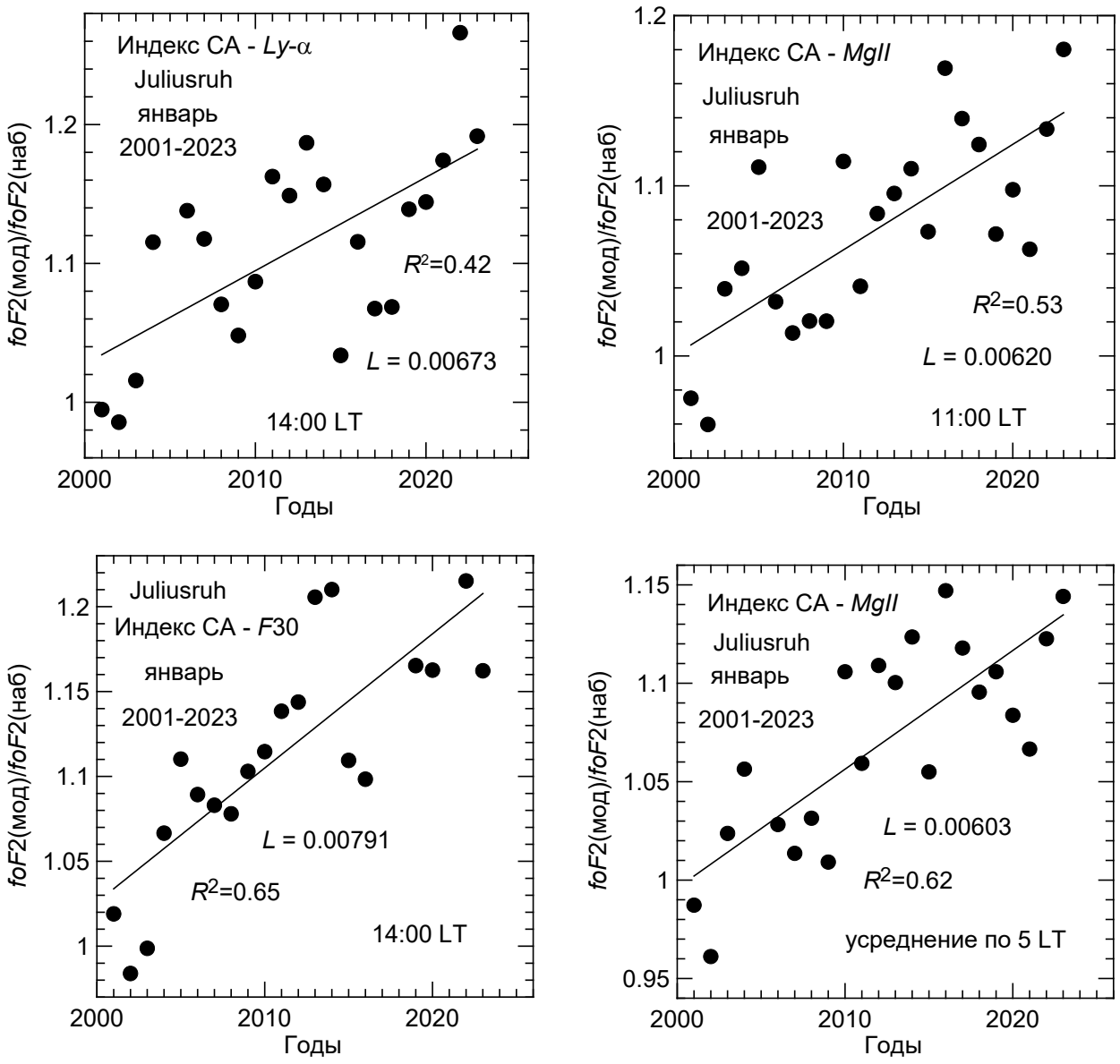
Индекс СА - Ly-α
Juliusruh
январь
2001-2023
R2=0.42
L = 0.00673
14:00 LT
foF2(мод)/foF2(наб)
Годы
Индекс СА - MgII
Juliusruh
январь
2001-2023
R2=0.53
L = 0.00620
11:00 LT
Juliusruh
Индекс СА - F30
январь
2001-2023
L = 0.00791
R2=0.65
14:00 LT
Индекс СА - MgII
Juliusruh
январь
2001-2023
L = 0.00603
R2=0.62
усреднение по 5 LT

Fig. 4.

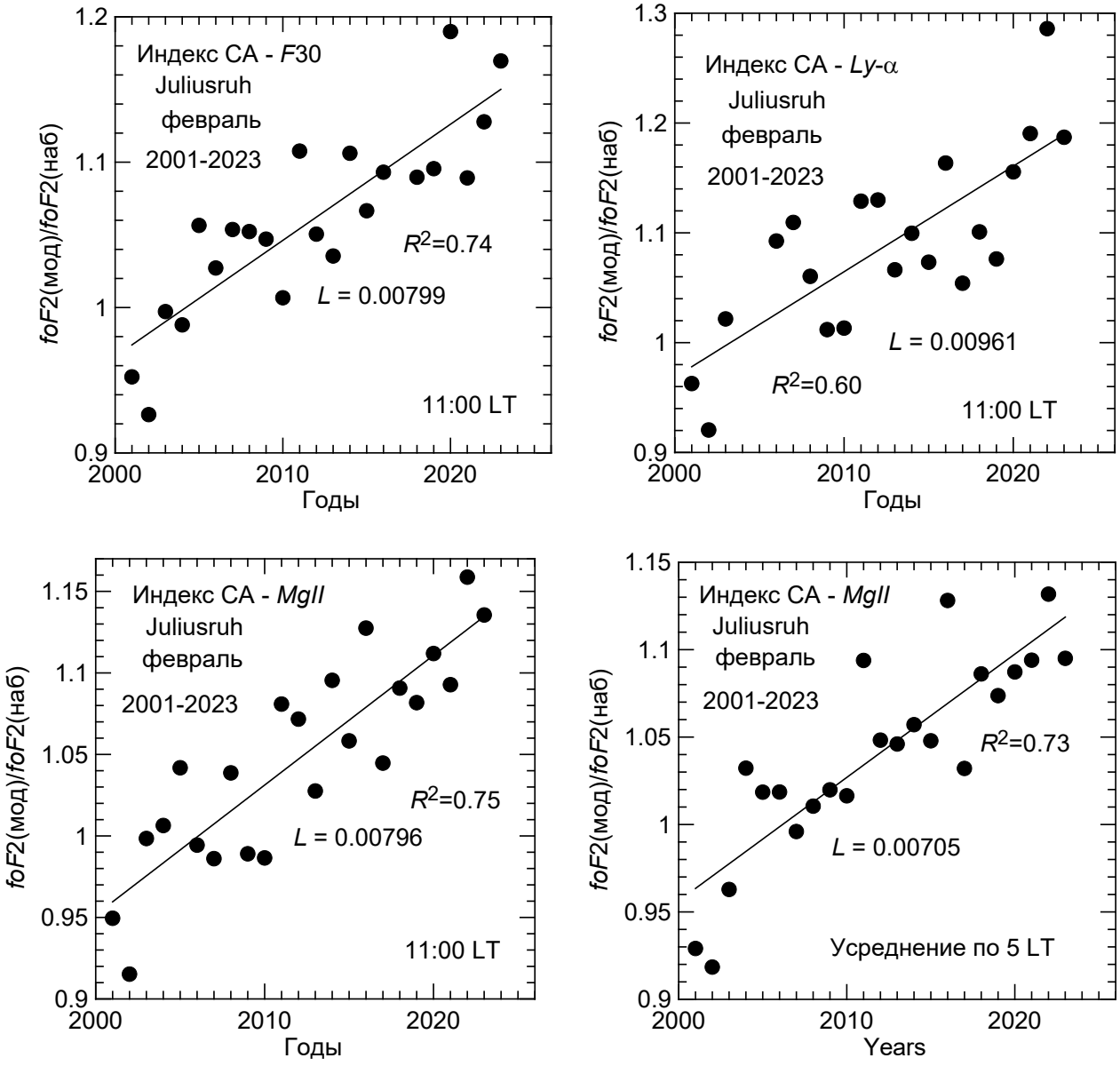
Индекс СА - F30
Juliusruh
февраль
2001-2023
R2=0.74
L = 0.00799
11:00 LT
foF2(мод)/foF2(наб)
Годы
Индекс СА - Ly-α
Juliusruh
февраль
2001-2023
L = 0.00961
R2=0.60
11:00 LT
foF2(мод)/foF2(наб)
Годы
Индекс СА - MgII
Juliusruh
февраль
2001-2023
R2=0.75
L = 0.00796
11:00 LT
foF2(мод)/foF2(наб)
Годы
Индекс СА - MgII
Juliusruh
февраль
2001-2023
R2=0.73
L = 0.00705
Усреднение по 5 LT
foF2(мод)/foF2(наб)
Years

Fig. 5.

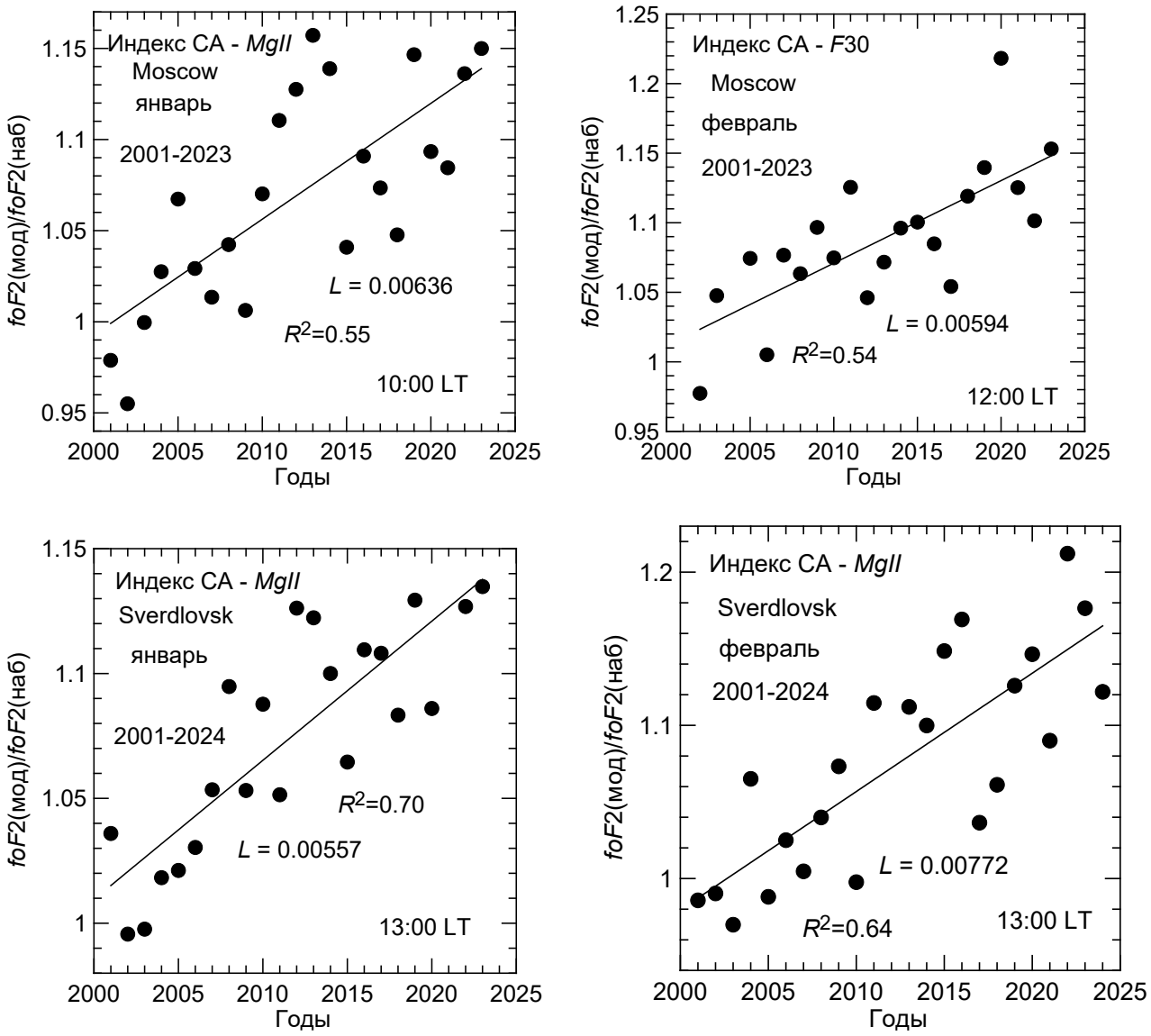
Индекс СА - MgII
Moscow
январь
2001-2023
L = 0.00636
R2=0.55
10:00 LT
foF2(мод)/foF2(наб)
Годы
Индекс СА - F30
Moscow
февраль
2001-2023
L = 0.00594
R2=0.54
12:00 LT
Индекс СА - MgII
Sverdlovsk
январь
2001-2024
R2=0.70
L = 0.00557
13:00 LT
Индекс СА - MgII
Sverdlovsk
февраль
2001-2024
L = 0.00772
R2=0.64
13:00 LT

Fig. 6.

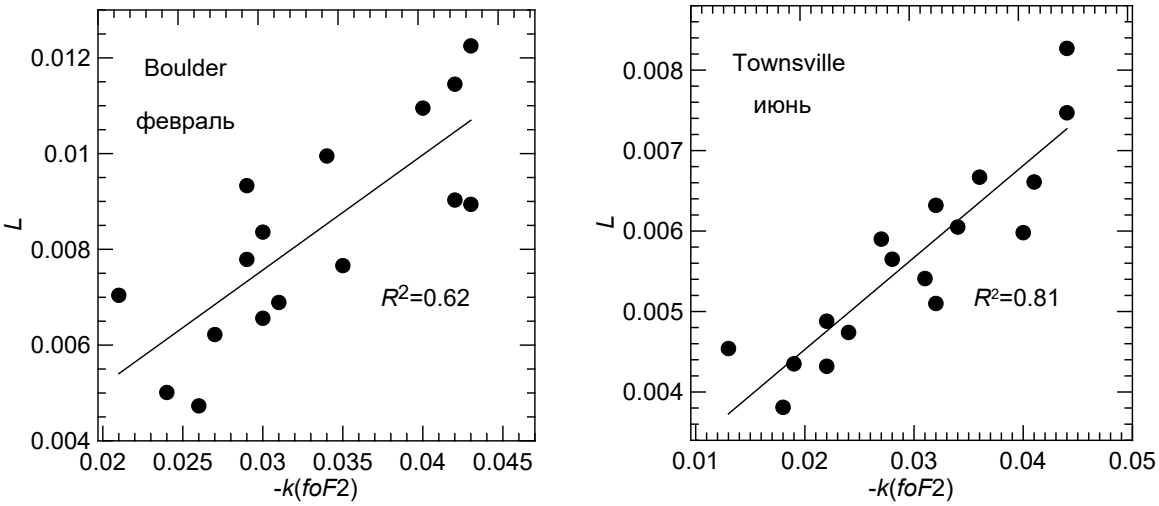
Boulder
февраль
R2=0.62
L
-k(foF2)
Townsville
июнь
R2=0.81

Fig. 7.